# Three-body decays and *R*-matrix analyses

H. O. U. Fynbo, R. Álvarez-Rodríguez,* A. S. Jensen, O. S. Kirsebom, and D. V. Fedorov
*Department of Physics and Astronomy, University of Aarhus, DK-8000 Aarhus C, Denmark*

E. Garrido
*Instituto de Estructura de la Materia, CSIC, Serrano 123, E-28006 Madrid, Spain*
(Received 10 March 2009; published 28 May 2009)

The *R*-matrix simulation of three-body decays is investigated as function of available $Q$ value and the energy and width of the intermediate two-body resonance. We use three $\alpha$-decaying unnatural parity states of $^{12}$C for illustration. The energy distributions are shown to be sensitive to the parameters when the two-body energy is significantly smaller than $Q$ and the width is smaller than about 0.5 MeV. The sequential decay inherent in the *R*-matrix formalism can then be distinguished from direct decay. We provide conditions for the validity of *R*-matrix analyses. We compare with full three-body computations of the same energy distributions where we also attempt to distinguish between sequential and direct decays. The results give a good reproduction of available experimental data and are consistent with the conclusions from *R*-matrix analyses. Nodes in the momentum distributions arise from angular momentum and parity conservation. Combined with symmetry requirements this constrains the momentum distributions significantly in some cases. Effects of interactions and decay mechanisms can only be seen in the remaining behavior as, e.g., additional nodes related to nodes in the coordinate wave function at large distance.

DOI: 10.1103/PhysRevC.79.054009 PACS number(s): 21.45.−v, 21.60.Gx, 25.70.Ef, 27.20.+n

## I. INTRODUCTION

Precise and kinematically complete experimental information is now available for a number of systems where a resonance breaks up into three or more fragments. The objectives for these activities are to uncover the structure of various nuclear systems, often nuclei far from stability or resonances close to cluster emission thresholds. The reaction, or decay, mechanism of these states is also of interest, both in itself as the dynamic behavior of the system and because the initial structure cannot be extracted without this knowledge. Due to the large binding energy of the $\alpha$ particle the threshold for one or more $\alpha$ particles is often low in light nuclei and therefore breakup to final states of three $\alpha$ particles or nucleons is experimentally easy to reach, e.g. breakup of $^{12}$C($3\alpha$), $^{9}$Be($2\alpha n$), $^{9}$B($2\alpha p$), $^{6}$He($\alpha 2n$), $^{6}$Li($\alpha pn$), $^{6}$Be($\alpha 2p$).

The number of such investigations is increasing due to the many new and upgraded operating facilities using unstable beams. Due to improvements in detection technologies these investigations often provide complete kinematics data. The accumulating sets of data are almost in all cases analyzed by *R*-matrix theory [1]. This method assumes two successive two-body processes that are used to reproduce the measured momentum distributions of the three fragments. The input is the properties of the intermediate states, resonance energies and widths, and initial population of the nuclear many-body system approximated as a three-body system at the surface of the nucleus. This implies that the results are information about the initial state obtained through these specific two-body decay or reaction channels.

The intermediate two-body structures are then important results of the analyses. They are expressed as branching ratios of such sequential decays. However, these two-body structures are unstable and together with the third cluster they are in reality states within the three-body continuum. It is then of both conceptual and practical interest to know whether this procedure is too restrictive and perhaps missing decay paths passing other configurations. After all, the paths via the two-body intermediate states are not direct observables and quantum mechanically a coherent sum of all possible paths applies.

Traditionally the nonsequential decays are called direct decays into the final states of the three-body continuum. Decays with no visible effects similar to sequential decay have also been called democratic decay [2,3]. The distinction between sequential and direct decays is not unique. In fact both descriptions can be correct as understood by expressing that the intermediate states serve as a basis. If the basis of two-body states multiplied by Coulomb waves for the third cluster is as complete as the set of continuum three-body wave functions then the choice of basis is a matter of convenience for example due to fast convergence. The task of extracting information about the initial structure requires at some point model interpretation.

The breakup of the $1^+$ state at 12.71 MeV in $^{12}$C provides a good example of the problems discussed. Parity conservation prevents the state from decaying sequentially by $\alpha$ emission to the narrow $0^+$ ground state of $^{8}$Be. In the literature, the three characteristic peaks from the breakup of this state have been described as signatures of both sequential [4–6] and direct [3,7] breakup.

The use of *R*-matrix theory for calculating the width of three-body decays has been discussed recently [8,9]. The purpose of the present article is to establish validity conditions

*Present address: INFN Sezione di Pisa. Largo Pontecorvo 3, I-56127 Pisa, Italy.

 

and predictive power for $R$-matrix calculations of decay spectra of three-body decays, when can it be used, and that predictions are reliable. Decay spectra is a more sensitive observable than the width alone, and it is also needed to separate possible sequential and direct contributions to the total width in the cases where such a separation might be possible.

We compare $R$-matrix calculations with a three-body model based on the method of hyperspherical adiabatic expansion combined with complex scaling. The discussion will be based on three unnatural parity states in $^{12}$C. Section II gives the pertinent background for the theoretical description of the three-body model and the method of $R$-matrix simulation. In Sec. III we discuss the constraints on the fragment momentum distributions from fermion and boson symmetry and from angular momentum and parity conservation. We give a number of numerical results for $^{12}$C resonances from $R$-matrix analysis in Sec. IV and from the three-body model in Sec. V. The reliability of the interpretations is discussed in Sec. VI and finally Sec. VII contains summary and conclusions.

## II. THEORETICAL BACKGROUND

Experimental analyses of three-body decays employ the $R$-matrix formalism that originally was developed for decays into two particles. We describe the modification in recent three-body applications and we sketch the physics content and parameter interpretation of this method. The results are structure parameters for the decaying systems and the decay mechanism expressed in terms of branching ratios of the decay via different known resonance properties of intermediate two-body systems. The data for the analyses leading to these results are momentum distributions of the three fragments. To explore the validity of this approximation we compare $R$-matrix calculations to proper three-body calculations. We sketch in the next subsection the important ingredients in this formalism that also sometimes allows distinction between different decaying initial structures and decay mechanisms.

### A. Three-body formulation

The aim is to compute the fragment momentum distributions from three-body decaying resonances. We define a resonance as a state with energy $E_{3r} - i\Gamma_{3r}/2$ corresponding to a pole of the $S$ matrix. This concept arises from an analytic continuation of the scattering matrix into the plane of complex energies. The pole can never be reached experimentally where the total energy only assumes real values. The imaginary part of the energy $-\Gamma_{3r}/2$ corresponds to a distribution of width $\Gamma_{3r}$ of these real energies around a peak value close to $E_{3r}$. The resonance wave function then includes effects of this distribution in total energy.

The resonances are calculated by the hyperspherical adiabatic expansion method [10] combined with complex rotation of the coordinates [11]. The adiabatic coordinate is the hyperradius $\rho$ defined by $m\rho^2 = \sum_{i<j} m_i m_j (\boldsymbol{r}_i - \boldsymbol{r}_j)^2/M$, where $M = m_i + m_k + m_j$ and $m$ is a normalization mass. The total wave function, $\Psi^{JM}$, is expanded on the angular eigenfunctions, $\Phi_{nJM}$, for each hyperradius, i.e.,

$$\Psi^{JM}(\rho, \Omega) = \frac{1}{\rho^{5/2}} \sum_n f_n(\rho) \Phi_{nJM}(\rho, \Omega), \tag{1}$$

where the $\rho$-dependent expansion coefficients, $f_n(\rho)$, are the hyperradial wave functions with the asymptotics $\exp(+i\kappa\rho)(\frac{\hbar^2\kappa^2}{2m} = E_{3r} - i\Gamma_{3r}/2)$ obtained from the coupled set of hyperradial equations. The necessary structures can be described from Borromean systems to systems with bound two-body states in one or more of the three two-body subsystems. The difficulties are often related to large distances (large $\rho$) that can be calculated accurately with a specific choice of basis and partial waves [12].

The Fourier transform providing the observable momentum distributions is almost entirely determined by the large-distance structure of the resonance coordinate wave function. The angular part is the same in momentum space and the momentum distributions are determined by

$$P \propto \frac{|\Psi^{JM}(\rho_{\max}, \Omega_k)|^2}{(E_{3r} - E)^2 + \Gamma^2/4}, \tag{2}$$

where $\Omega_k$ specify the directions of the relative momenta in hyperspherical coordinates. The wave function has to be evaluated at $\rho_{\max}$ where the asymptotic $\rho$ dependence of $f_n(\rho) \propto \exp(i\kappa\rho)$ has been reached. The energy distributions from the three-body decaying resonances are then obtained from the large-distance asymptotic behavior of the three-body resonance wave function [13]. The complex rotation of the coordinates in the Faddeev equation is described by $\rho \rightarrow \rho \exp(i\theta)$. In hyperspherical coordinates this means that only the hyperradius $\rho$ is scaled as $\rho \rightarrow \rho \exp(i\theta)$ while all hyperangles remain unchanged. The angle $\theta$ has to be larger than the angle $\theta_{3r}$ corresponding to the resonance, i.e., $\theta > \theta_{3r} \equiv 0.5 \arctan(\Gamma_{3r}/2E_{3r})$, where $E_{3r}$ is the energy and $\Gamma_{3r}$ is the width. Then the resonance wave function falls off exponentially at large distance precisely as a bound state.

The adiabatic expansion implies that the asymptotic large-distance population of different adiabatic components are available. Each of these components describes specific continuum structures of the three-body system. In particular, one of these wave functions must asymptotically describe one particle far away from the other two in the two-body resonance structure. This happens as soon as $\theta$ is larger than $\theta_{2r} \equiv 0.5 \arctan(\Gamma_{2r}/2E_{2r})$, the angle corresponding to that resonance of energy and width $E_{2r}$ and $\Gamma_{2r}$. The fraction populating this resonance is related to the size of the radial wave function, $f_n(\rho)$, of that component. We define this fraction as the part decaying sequentially through the corresponding two-body structure. Several such components may be present in addition to the majority of adiabatic components describing genuine three-body continuum properties with the corresponding direct decay mechanism.

In contrast to the direct decays, momentum distributions arising from the sequential components cannot be obtained from the complex rotated wave function at large distance. This is because these structures really are bound states in the complex rotated basis. Rotation back to the real axis

recreates a decaying two-body resonance of given energy and width. Combined with energy and momentum conservation including the third particle the decay can then be described as a genuine two-body sequential decay where the third particle has escaped and does not interact with the particles in the decaying two-body resonance. In the lowest-order approximation this means simply a Breit-Wigner distribution for the third particle around the most probable energy and a width equal to the sum of two and three-body resonance widths. If the third particle and the particles forming the two-body resonance are identical, corresponding amplitude contributions must be coherently added and squared. Finally, the different contributions to the momentum distributions from direct and sequential decays should then be individually computed and added. It is not clear whether this should be done coherently or incoherently as discussed in detail in Refs. [8,9].

When the lowest-order Breit-Wigner approximation is insufficient this procedure is inadequate, i.e., when $\Gamma_{2r}$ becomes too large. When $\Gamma_{2r}$ is comparable to $E_{3r}$ (assumed larger than $E_{2r}$) the concept of three-body sequential decay through this state looses its meaning because the energy of the first emitted particle vary too much to allow a description in terms of one energy and one potential (barrier). The separation of degrees of freedom into sequential and direct decays is not possible. This restriction in widths is less severe for $\Gamma_{3r}$ because the distribution of particle momenta first of all is determined by the resonance wave function while the smearing due to the width either is of rather little significance or easily can be accounted for.

When the two-body resonance energy is larger than the three-body energy, $E_{2r} > E_{3r}$, energy conservation does not allow this sequential decay mechanism. However, the decay may proceed by first establishing a similar intermediate structure with one particle far away from two particles in a resonance-like structure, and then at much larger distances depopulating this component while reaching the true asymptotic behavior allowed by energy conservation. This is called virtual sequential decay, which qualitatively resembles the phenomenological description in analysis of decay via the tail of a two-body resonance. The virtual sequential decay also qualitatively resembles the results from calculations with $\theta < \theta_{2r}$ where the two-body resonance is spread out over many three-body continuum states instead of appearing as one state with bound state boundary condition. The complete momentum distributions including direct and virtual sequential decays are obtained provided the asymptotic behavior can be accurately computed.

### B. $R$-matrix formulation

$R$-matrix theory [1] is the most frequently applied formalism for a phenomenological description of data. For decay to two-body final states the assumption is that space can be divided into an inner region, where strong forces are active, and an outer region, where only Coulomb and angular momentum determine the wave function. The two regions of space are then connected at the interface of the two regions by specifying values of reduced width and energy parameters.

For decay to three-body final states the assumption is that such decays can be seen as a succession of two two-body decays (sequential decay), i.e., emission of one particle leading to population of an intermediate two-body structure that subsequently decays. The total energy can then be shared in different proportion between the three particles. If several sequential decays are possible the total decay is described as a sum of the individual channels. Lane and Thomas discuss the validity conditions of $R$-matrix theory for such decays [1], most notably the requirement is that the lifetime of the intermediate state is sufficiently long to allow a correct description of the outer region in the first decay in terms of two-body asymptotics depending only on Coulomb and angular momentum.

$R$-matrix theory can be adjusted to handle more complex situations such as (i) several paths related to different angular momentum couplings but the same intermediate state, (ii) different interfering intermediate structures for the same two-body system, and (iii) coherence of intermediate structures of different two-body systems.

As our chosen example we consider three-$\alpha$ decays of $^{12}$C resonances of energy $E_{3r}$. When the intermediate state is the ground state of $^{8}$Be with a lifetime of the order $10^{-16}$s (width about 8 eV) the two successive two-body decays seem to be appropriate, i.e., $^{12}\mathrm{C} \rightarrow \alpha_1 + {}^{8}\mathrm{Be} \rightarrow \alpha_1 + \alpha_2 + \alpha_3$. The kinematics is fully determined by specifying the relative energy of the $^{8}$Be system, $E_2$, and the angle $\Theta$ between the directions of the first emitted $\alpha$ particle and the direction of the subsequent breakup of $^{8}$Be. The distribution of $E_2$, or that of the first $\alpha$ particle $E_{\alpha 1} = \frac{2}{3}(E_{3r} - E_2)$, is given by $|f_{1,23}|^2$ with

$$f_{1,23} \propto \frac{\sqrt{\Gamma_1 \Gamma_2 / \sqrt{E_{\alpha 1} E_2}}}{E_{2r} - \gamma_2^2 [S_{\ell_x}(E_2) - S_{\ell_x}(E_{2r})] - E_2 - i\frac{1}{2}\Gamma_{2r}}, \quad (3)$$

where $\Gamma = 2P_\ell(E)\gamma^2$ with $P_\ell(E)$ the penetrability for either the $\alpha$-$^{8}$Be ($\Gamma_1$) or $\alpha$-$\alpha$($\Gamma_{2r}$) breakup, $\gamma^2$ is the reduced width and $S_\ell$ is the shift function [5,6]. $E_{2r}$ is the formal resonance energy in $^{8}$Be. The orbital angular momentum is $\ell_y$ for the first emission and $\ell_x$ for the $^{8}$Be state.

When $^{8}$Be is in its ground state the validity conditions for successive emissions are obeyed to a high precision. In contrast, these requirements seem to be violated when the intermediate state is the $^{8}$Be($2^+$) state at 3 MeV with a width of $\Gamma_{2r} \approx 1.5$ MeV. Somewhat surprisingly, such decays have also been successfully described by $R$-matrix theory. An example of this is provided by the $1^+$ state at 12.71 MeV in $^{12}$C [5,6] where $\ell_y = 2$ and $\ell_x = 2$ in Eq. (3). The distribution of $\Theta$ can be calculated from Ref. [14] to be $W(\Theta) = \sin^2(2\Theta)$. Then three peaks results for the energy distribution with the central peak dominated by the first emitted $\alpha$ particle while the other two peaks originate from the secondary emitted $\alpha$ particles. The angular correlation $W(\Theta)$ determines the shape of these peaks.

The distribution given by Eq. (3) neglects the Bose symmetry of the three $\alpha$ particles. The resulting interference effects have to be taken into account. This was pointed out for the decay spectrum of the 12.71-MeV state in Ref. [5] where a

modified $R$-matrix expression was given (Eq. (3) in Ref. [5]),

$$f = \sum_{m_x \ell_y} (\ell_y M - m_x j_x m_x | J M) Y_{\ell_y}^{M-m_x}(\Theta_y, \Phi_y) \times Y_{\ell_x}^{m_x}(\theta_x, \phi_x) f_{1,23}\, e^{i(\omega_{\ell_y} - \phi_{\ell_y})} e^{i(\omega_{\ell_x} - \phi_{\ell_x})}, \quad (4)$$

where $(\Theta_y, \Phi_y)$ is the direction of emission of the first $\alpha$ particle in the $^{12}$C center-of-mass, $(\theta_x, \phi_x)$ the direction of one of the secondary emissions in the $^{8}$Be center-of-mass, $J$ and $j_x$ are the total angular momenta of the states in $^{12}$C and $^{8}$Be, and $\omega_\ell - \phi_\ell$ is the Coulomb minus hard sphere phase shift. The summation over $\ell_y$ is active when more than one value is allowed by the coupling rules. The final amplitude is obtained by symmetrizing in the coordinates of the three $\alpha$ particles, then squaring and finally averaging over the initial spin direction $M$. Due to this procedure interference effects are introduced.

For the $1^+$ state in $^{12}$C the effect of this interference is to deepen the minima between the three peaks such that the agreement with the data is significantly improved [5,6].

## III. SYMMETRY CONSTRAINTS

The decaying structure may be a resonance or other continuum stare at small distance evolving into three clusters at large distance.

In any case the structure can be described by a linear combination of a basis set of quantum numbers. When some of the quantum numbers are conserved, as for a resonance with given angular momentum and parity $J^\pi$, the momentum distributions are constrained accordingly. Furthermore, the boson or fermion symmetry of the constituent clusters also imposes constraints on the resulting momentum distributions as already discussed in the $R$-matrix formulation.

For both data and the computed wave function the constraints from conservation laws and symmetry requirements can be exhibited in Dalitz plots [15]. For the three-$\alpha$ decay of $^{12}$C knowledge of two $\alpha$ energies suffices to uniquely specify the $3\alpha$ final state. It can be visualized by points inside an equilateral triangle, where the distances to the sides are the energies of the three particles, see Fig. 1. The density of the Dalitz plot is then proportional to the transition matrix element squared. Pure phase-space decays, where the wave function is independent of the momenta, result in a flat distribution. Symmetries derived from angular momentum and parity conservation as well as boson symmetry induce general structures in the Dalitz plots. In addition, specific structures arise due to interactions between the $\alpha$ particles, e.g., leading to a $^{8}$Be resonance. These two types of structures are distinctly different as the first is of static origin, whereas the second carries information about the decay mechanism.

An early example of the effects of symmetries was found in three-pion decays studied by C. Zemach [16]. Solely on the grounds of Bose statistics and conservation of spin, isospin, and parity, and assuming a nonpolarized initial state, he was able to show that the transition matrix element takes on certain general forms depending on the spin, isospin, and parity of the system forcing the density to vanish in certain regions of the

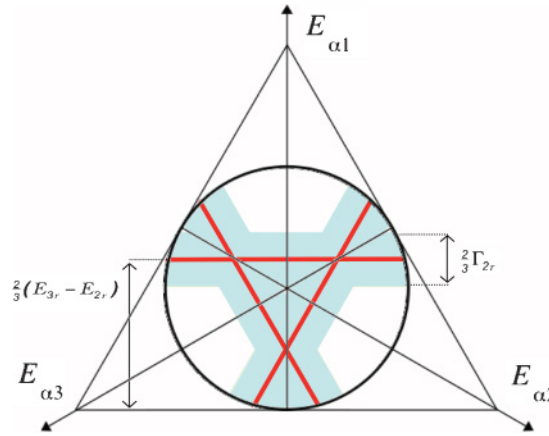


FIG. 1. (Color online) Density structures of the Dalitz plot for sequential decays. The inscribed circle marks the boundary of the kinematically allowed region.

Dalitz plot. No assumptions about the interactions involved are needed except that they have to conserve isospin and parity. Pions and $\alpha$ particles are both spin-zero bosons but have opposite parities (negative and positive, respectively) and, in contrast to $\alpha$ particles, pions possess a nonzero isospin of $I = 1$. The formulations of Ref. [16] for three-pions can readily be applied to $3\alpha$ decays as long as we account for the difference in parity and use the results for the totally symmetric isospin state of $I = 3$.

The results are shown in Fig. 2. The natural parity states $[\pi = (-1)^J]$ in the left column turn out to have rather few nodes in the distributions due to symmetry constraints. In contrast the unnatural parity states $[\pi = (-1)^{J+1}]$ in the right column show many points and curves of vanishing probability.

These nodes and the conserved quantum numbers are known to be present from population to detection. Obviously many nodes and a characteristic pattern facilitate enormously the spin-parity assignment of decaying resonances. Theoretical predictions may also be deceivingly close to measurements provided the correct symmetry constraints are obeyed.

It should be emphasized that other nodes in measured distributions only signal structures of the decaying resonances at intermediate or large distances. The relation to the small-distance behavior, where the characteristic large amplitude structure is present, can only be through models.

In this connection it is revealing to look at the free wave functions obtained for three particles without interactions, but with the correct symmetries [2,3] (referred to as democratic decay in the literature). The hyperspherical angular solution $\Phi(\rho, \Omega)$ for short-range potentials is identical for $\rho = 0$ and $\rho = \infty$. Thus, in this case the small- and large-distance structure cannot be distinguished and the measured distributions would directly reflect the characteristic bulk structure at small distance. If, furthermore, a number of nodes are present like for the decay of $^{12}$C$(1^+)$ this rather crude approximation is successful although it basically only reflects the conserved quantum numbers; see Fig. 3. This success is also to some extent maintained for the $^{12}$C$(2^-, 4^-)$ decaying states where the constraints are less severe than for $1^+$, see Fig. 2.

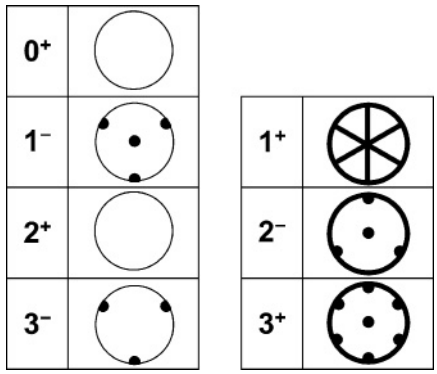


FIG. 2. Regions of the $3\alpha$ Dalitz plot where the density must vanish are shown in black. The vanishing is of higher order where the black lines and dots overlap. The pattern for a spin $J + 2n(n = 1, 2, 3, \ldots)$ is identical to the pattern for spin $J$ (provided $J \geqslant 2$) except that the vanishing at the center is not required for spins $\geqslant 4$. The equilateral triangle of the Dalitz plots are not shown; see Fig. 1.

When only few constraints from symmetry are present the effects of interactions and the related decay mechanisms are more pronounced in the Dalitz plots.

## IV. RESULTS FROM $R$ MATRIX

We choose $^{12}$C states below the proton emission threshold to illustrate the simulations obtained with the $R$-matrix formalism. These states are only energetically allowed to decay into three $\alpha$-particles or by photon emission. For natural-parity states the intermediate $^8$Be two-body state reached after emission of one $\alpha$ particle can be any of the $^8$Be excited states. The $0^+$ state could then be expected to be the dominating decay path with smaller contributions from $2^+$. The unnatural parity states can in contrast not decay via the $^8$Be $0^+$ state. The $2^+$ state is then expected to be the dominating decay path. The $4^+$ state at much higher energy probably would be negligibly small for the chosen low-lying $^{12}$C resonances. To have a clean simulation we therefore select unnatural parity states and ignore the $4^+$ contribution. The structure and decays of $^{12}$C are recently investigated and described in [7,17–19]. The $2^+$ energy is $E_{2r} = 2.7$ MeV above the threshold for separation into two free $\alpha$-particles and the width is $\Gamma_{2r} = 1.5$ MeV.

Qualitatively, the density of the Dalitz plot will have the structure shown on Fig. 1. One $\alpha$ particle is emitted with $2/3$ of the available energy $E_{3r} - E_{2r}$ while the energies of the remaining two particles depend on the orientation of the two-body decay relative to the trajectory of the first particle. This gives rise to three straight lines running parallel to the sides of the equilateral triangle at a distance of $\frac{2}{3}(E_{3r} - E_{2r})$. A finite width in the intermediate $^8$Be resonance will be seen as a broadening of these lines into bands of finite width. Their lateral structure depends on the resonance shape and barrier penetration while the longitudinal structure is determined by the angular correlations in the decay. Depending on the position and width of the resonance the bands may overlap leading to destructive or constructive interference in accordance with the node structure discussed in Sec. III.

### A. Dependence on $R$-matrix parameters

The $1^+$ state in $^{12}$C appears at $E_{3r} = 5.43$ MeV above the threshold for three free $\alpha$-particles with a partial width of $\Gamma_{3r} = 18.1$ eV. This resonance is very narrow and represents a successful example of an $R$-matrix analysis of a detailed and accurate set of measured data. The small width implies that the only important quantities are the two-body energy and width measured in units of the three-body energy, i.e., $E_{2r}/E_{3r}$ and $\Gamma_{2r}/E_{3r}$ that are known experimentally to be 0.497 and 0.276, respectively.

We vary the two-body energy and width measured in units of the three-body energy; see fig. 4. The Dalitz distribution is then computed from Eq. (3) averaged over initial state $m$ states and squared, i.e., the probability for populating different regions of the phase-space of three $\alpha$ particles. We normalize the $\alpha$-particle energies to the maximum allowed by energy conservation. The picture is emission of one $\alpha$ particle and occupation of the $2^+$ state in $^8$Be that in turn decays into two $\alpha$ particles. Then the relative angular momentum between the first emitted $\alpha$ particle and $^8$Be is $\ell_y = 2$. We also give the single-$\alpha$ energy distribution obtained by projecting on the vertical axis on the Dalitz plot. This distribution gets contributions from all the three identical decay products.

In the lower left corner of Fig. 4 both the two-body energy and width are rather small. The narrow peak at 0.55 arises from emission of the first $\alpha$ particle and the other broader

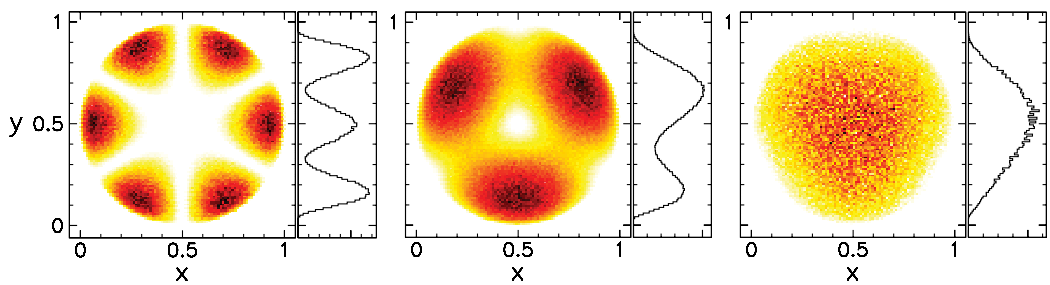


FIG. 3. (Color online) The computed dalitz distribution for decays of the $^{12}$C resonances with spin-parity $1^+, 2^-, 4^-$, respectively. The distributions are obtained with the lowest hyperspherical wave function with the correct angular momentum and parity. The coordinates are $y = E_{\alpha 1}$ and $x = \frac{E_{\alpha 1}+2E_{\alpha 2}}{\sqrt{3}} + \frac{1-\sqrt{3}}{2}$ with the energies normalized to the maximal possible $\alpha$ energy $E_{\alpha,\max} = 2E_{3r}/3$. The single $\alpha$-energy distributions are shown as projections on the ordinate axis.

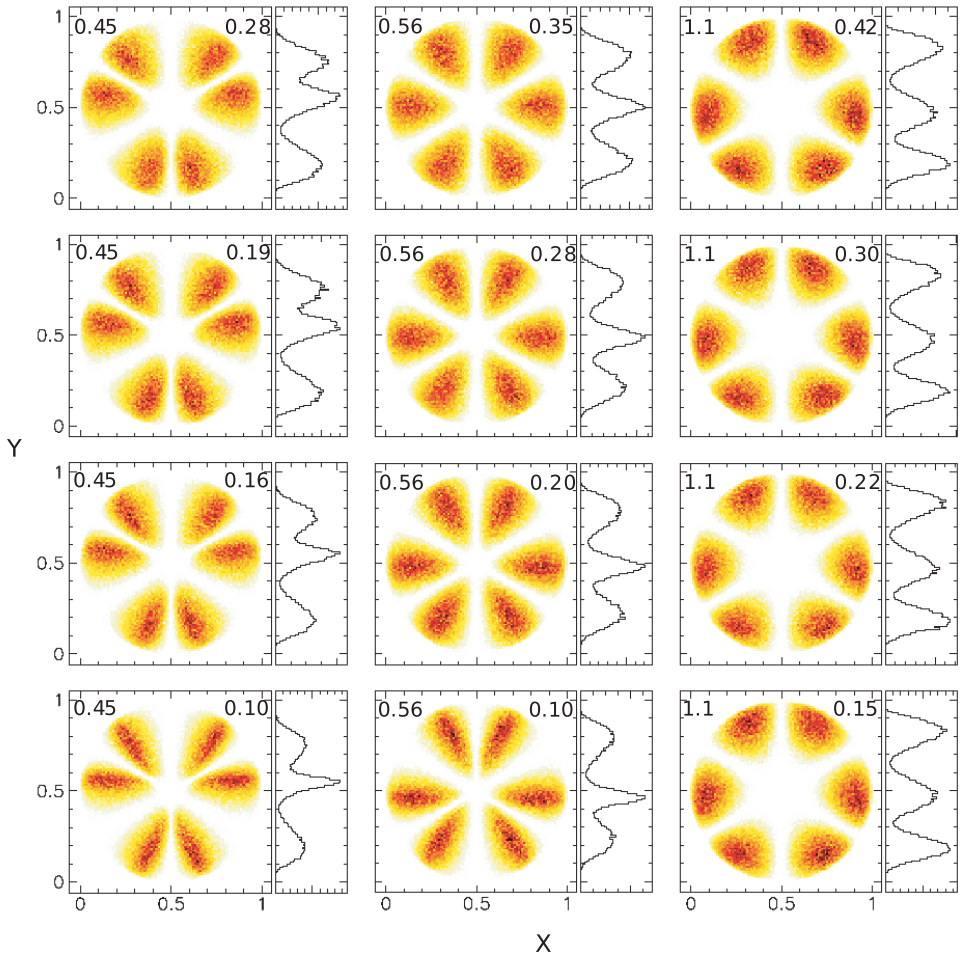


FIG. 4. (Color online) Dalitz distributions from $R$-matrix analysis for decay into three $\alpha$-particles of the $1^+$ resonance in $^{12}$C at an energy of $E_{3r} = 5.43$ MeV and a partial width of about 18.1 eV. The energies and widths of the intermediate $2^+$ resonance in $^8$Be are varied in the simulations. $E_{2r}/E_{3r}$ is given to the left and $\Gamma_{2r}/E_{3r}$ to the right in the panels. The single-$\alpha$ energy distributions are shown as projections on the ordinate axis. The coordinates are $y = E_{\alpha 1}$ and $x = \frac{E_{\alpha 1}+2E_{\alpha 2}}{\sqrt{3}} + \frac{1-\sqrt{3}}{2}$ with the energies normalized to the maximal possible $\alpha$ energy $E_{\alpha,\max} = 2E_{3r}/3$.

humps on both sides are from decay of $^8$Be. Increasing the width and maintaining the two-body energy is shown in the left panel of Fig. 4. The distribution of the first emitted particle is now broadened but remaining at the same position as the other two particles. The three-peak distribution becomes rather pronounced. If we instead increase the energy of the intermediate resonance by moving to the right in Fig. 4 the symmetric three-peak distribution emerges even when the two-body width is small. Increasing the width with $E_{2r} \approx E_{3r}$ essentially leaves the distribution unchanged. The overall conclusion is that the distribution is insensitive to the two-body parameters when $E_{2r}/E_{3r}$ is larger than about 0.5 depending somewhat on $\Gamma_{3r}/E_{3r}$.

The next unnatural parity state has $J^\pi = 2^-$ with energy $E_{3r} = 4.55$ MeV above the threshold and a partial width of $\Gamma_{3r} = 260$ keV. Then $E_{2r}/E_{3r}$ and $\Gamma_{2r}/E_{3r}$ are known experimentally to be 0.60 and 0.33, respectively. For this state complete kinematics data are still lacking. In this case two relative angular momenta between the first emitted $\alpha$-particle and $^8$Be are possible, $\ell_y = 1, 3$. Again we vary the two-body parameters in the $R$-matrix simulation and find the distributions in Figs. 5 and 6 for $\ell_y = 1, 3$, respectively. There is a tendency for more oscillations for the highest angular momentum. The lower left corner reveals the same feature as for $1^+$ of a narrow peak arising from emission of the first $\alpha$ particle. This peak is smeared out as the two-body width increases, and rather quickly traces of its origin have disappeared. The distributions become insensitive to the two-body parameters for all widths when $E_{2r}$ becomes comparable to $E_{3r}$ and for smaller values of $E_{2r}$ as soon as the width is moderate compared to $E_{3r}$.

We also investigated the unnatural parity state with $J^\pi = 4^-$ with energy $E_{3r} = 6.08$ MeV and width $\Gamma_{3r} = 375$ keV. This state comes out naturally in three-body computations but the experimental assignment is tentative. The values of $E_{2r}/E_{3r}$ and $\Gamma_{2r}/E_{3r}$ are 0.45 and 0.25, respectively. In this case the two possible relative angular momenta between the first emitted $\alpha$ particle and $^8$Be are $\ell_y = 3, 5$. The corresponding distributions again display the tendency of more oscillations for the highest angular momentum. The results of varying the two-body parameters in the $R$-matrix simulation are shown in Figs. 7 and 8 for the two values of the angular momentum. These distributions quantitatively resemble those of the $2^-$ state with the same features of insensitivity when either $E_{2r}$ or $\Gamma_{2r}$ are sufficiently large.

For all three cases Bose symmetry has a significant effect on the distributions as discussed in detail for the $1^+$ state in Refs. [5,6]. This is also clear from Fig. 2 where each of these states have nodes in significant parts of the Dalitz plot. When either $E_{2r}$ or $\Gamma_{2r}$ are sufficiently large the Dalitz plots are insensitive to $E_{2r}$ and $\Gamma_{2r}$ and they are instead mainly determined by the symmetry requirements.

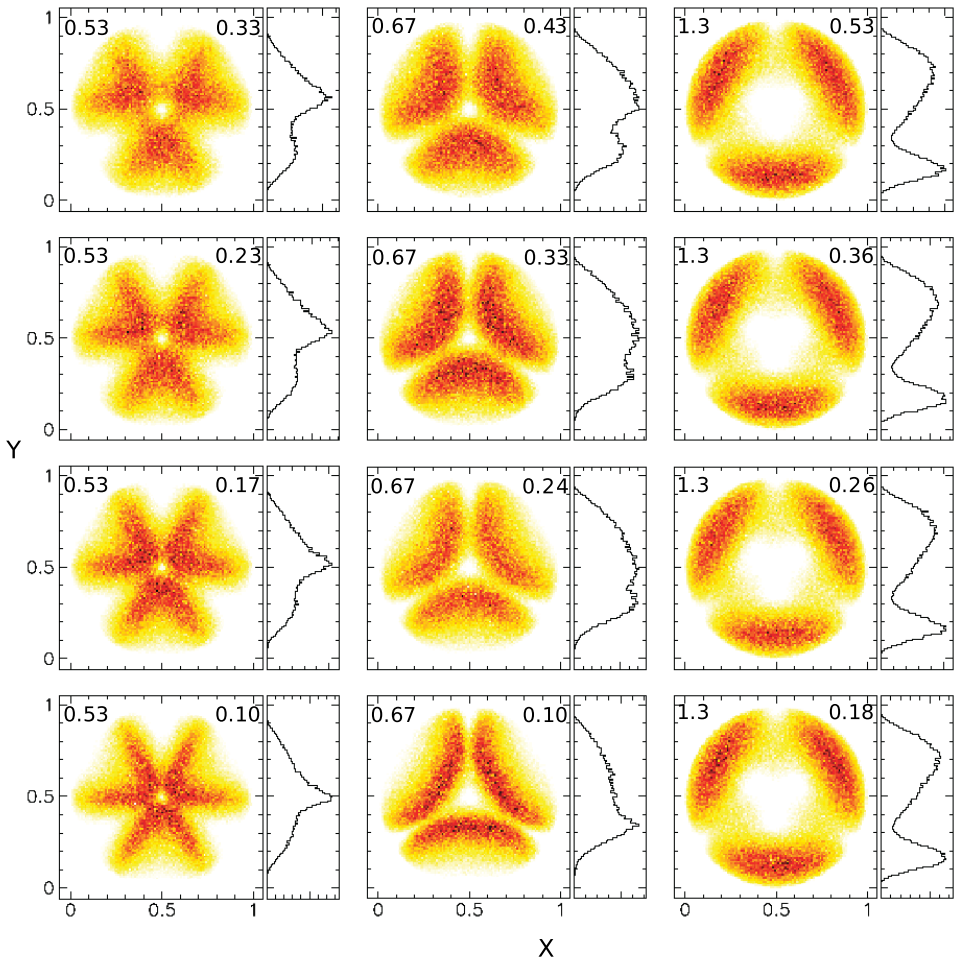


FIG. 5. (Color online) Dalitz distributions from $R$-matrix analysis for decay into three $\alpha$ particles of the $2^-$ resonance in $^{12}$C at an energy of $E_{3r} = 4.55$ MeV. The energies and widths of the intermediate $2^+$ resonance in $^8$Be are varied. $E_{2r}/E_{3r}$ is given to the left and $\Gamma_{2r}/E_{3r}$ to the right in the panels. The relative angular momenta between the first $\alpha$ particle and $^8$Be is $\ell_y = 1$. The coordinates are $y = E_{\alpha 1}$ and $x = \frac{E_{\alpha 1}+2E_{\alpha 2}}{\sqrt{3}} + \frac{1-\sqrt{3}}{2}$ with the energies normalized to the maximal possible $\alpha$ energy $E_{\alpha,\max} = 2E_{3r}/3$. The single-$\alpha$ energy distributions are shown as projections on the ordinate axis.

### B. The consistency of the concept of sequential decay

The $R$-matrix formalism applied to three-body decaying systems inherently uses intermediate two-body structures parametrized by energies and widths. Intuitively this is appealing for narrow structures accessible by ordinary particle emission. However, it becomes suspicious in two parameter regions. First, when the width of the intermediate structure corresponds to a short lifetime comparable to the time the first emitted particle needs to move outside the interaction range of the remaining two particles, then the second decay has taken place before or during the first emission populating the intermediate structure and the assumptions of $R$-matrix theory break down as discussed in Sec. II B.

Second, when energy conservation prohibits population of the intermediate structures, then explanations in terms of tails of these resonances are invoked to maintain energy conservation, but it does not explain the concept where an inaccessible state is populated and subsequently decays. This is the description independent of the width of the intermediate state that as well could approach zero. Then it is obvious that such a decay mechanism requires the concept of virtual population but this is not employed in the rather classical $R$-matrix formulation of two independent consecutive processes.

Interestingly our results in the previous subsection also indicate when the $R$-matrix analysis is lacking sensitivity. The insensitivity of the energy distributions toward parameter variations immediately demonstrates that accurate parameter values only can be deduced with care. Let us assume that the resonance energy $E_{3r}$ is attempted extracted from the data set where $E_{2r}$ and $\Gamma_{2r}$ are known. If either $E_{2r}$ or $\Gamma_{2r}$ are too large the simulated distributions would match the data for a large interval of $E_{3r}$ values. These two conditions are in perfect agreement with the two suspicious parameter regions mentioned above.

However, the insensitivity is only on the plots of probability against single-$\alpha$ energy measured relative to the maximum allowed. Because this maximum energy simply is two-thirds of $E_{3r}$ the largest measured single-$\alpha$ energy gives directly $E_{3r}$ with corresponding accuracy. Thus an attempt to determine $E_{2r}$ and $\Gamma_{2r}$ from the $R$-matrix analysis and this measured value of $E_{3r}$ could easily be very inaccurate. Fortunately such determination is usually not attempted.

The condition of large $E_{2r}$ or $\Gamma_{2r}$ can be expressed quantitatively by comparing the interaction range and the distance $s_a$ the first emitted particles move before the remaining two-body system decays. To estimate $s_a$ we multiply the velocity of the emitted particle relative to the remaining two-body system and the lifetime $\hbar/\Gamma_{2r}$. This gives

$$s_a \approx \frac{\hbar}{\Gamma_{2r}}\sqrt{\frac{4(E_{3r}-E_{2r})}{3m_a}} \approx \frac{7\text{ fm}}{\sqrt{A_a}}\sqrt{\frac{E_{3r}-E_{2r}}{1\text{ MeV}}}\frac{1\text{ MeV}}{\Gamma_{2r}}, \quad (5)$$

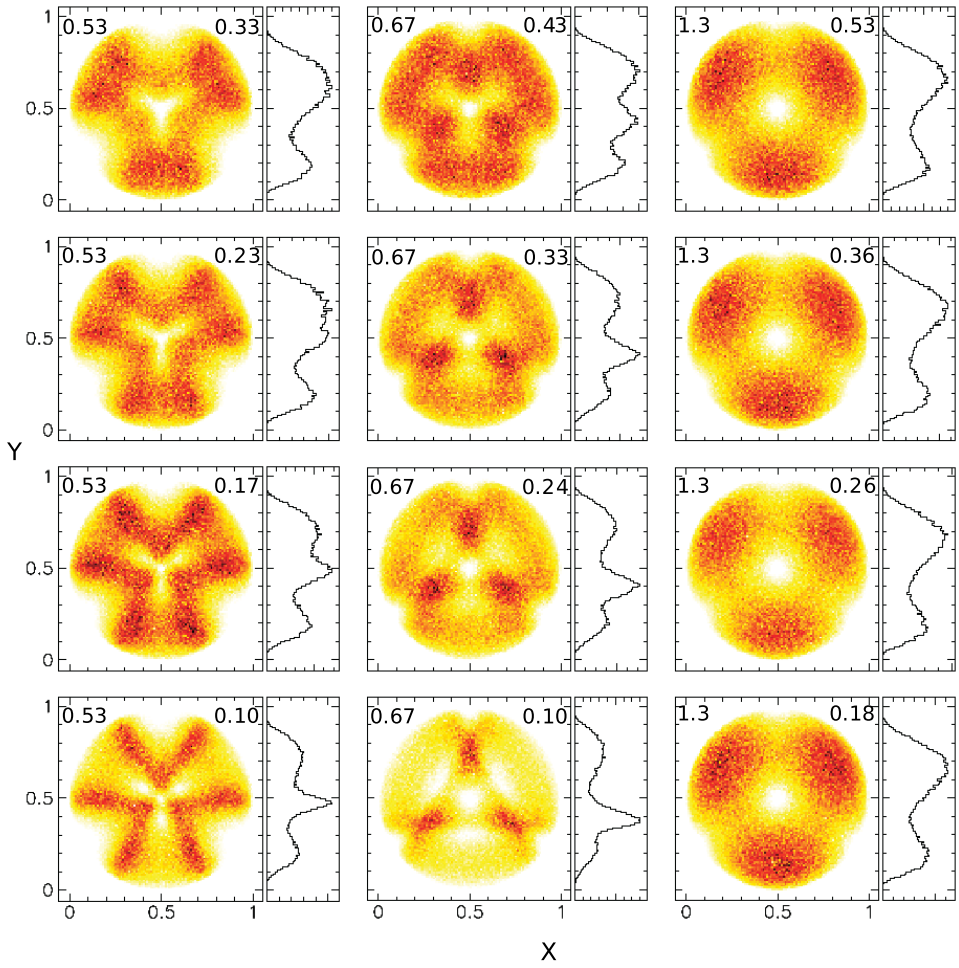


FIG. 6. (Color online) Dalitz distributions from $R$-matrix analysis for decay into three $\alpha$ particles of the $2^-$ resonance in $^{12}$C at an energy of $E_{3r} = 4.55$ MeV. The energies and widths of the intermediate $2^+$ resonance in $^8$Be are varied. $E_{2r}/E_{3r}$ is given to the left and $\Gamma_{2r}/E_{3r}$ to the right in the panels. The relative angular momenta between the first $\alpha$ particle and $^8$Be is $\ell_y = 3$. The coordinates are $y = E_{\alpha 1}$ and $x = \frac{E_{\alpha 1}+2E_{\alpha 2}}{\sqrt{3}} + \frac{1-\sqrt{3}}{2}$ with the energies normalized to the maximal possible $\alpha$ energy $E_{\alpha,\max} = 2E_{3r}/3$. The single-$\alpha$ energy distributions are shown as projections on the ordinate axis.

where $m_a \approx A_a m_n$ is the mass of the first emitted particle expressed in terms of neutron mass $m_n$ and nucleon number $A_a$. For low-lying resonances for light nuclei a rough estimate is $s_a \approx 2/\Gamma_{2r}$ that shows that the most decisive factor is the value of the width of the intermediate resonance $\Gamma_{2r}$. If the criterion is $s_a > 4$–$10$ fm (the radius of the constituent particle plus the interaction range plus distance between particles) we as a rule of thumb find must require at least that $\Gamma_{2r} < 0.2$–$0.5$ MeV. For larger values of $\Gamma_{2r}$ the sequential decay mechanism is ill defined. This is consistent with the above conclusions found by variation of the $R$-matrix simulations.

When this condition is violated, direct and sequential decays cannot be distinguished. This can be expressed by saying that all decays are direct because the intermediate structure has decayed before the first particle has left the interaction region. Similar considerations were formulated in an early article using $T$-matrix calculations [20]. When the condition is fulfilled this division is meaningful both theoretically and experimentally. The analysis can be carried out and the decay products can be kinematically selected to come from an intermediate structure. More than one sequential path may be possible for example through two-body resonances in different subsystems. Each of these paths should first fulfill the criterion. Second, it is necessary that the paths are mutually orthogonal for the deduction of branching ratios to be meaningful. The second condition is not obvious because the angular-momentum coupling schemes can be very different in different Jacobi systems, even when the total wave function is the same. Orthogonality is then only assured by other quantum numbers than angular momenta that almost inevitably implies that the spatial extension prevent any overlap. We then come back to the condition of sufficiently long lifetime.

## V. RESULTS FROM THREE-BODY COMPUTATIONS

Breakup energy distributions for the three $^{12}$C resonances are also computed in the three-body model described in Sec. II A. Details of the procedure and systematic results can be found in Ref. [19]. The basic input is the two-body $\alpha$-$\alpha$ potential for each of the contributing partial waves. These interactions are designed to reproduce the low-energy phase shifts or the two-body resonances for the angular momenta of the corresponding partial waves. In particular the $2^+$ parameters reproduce roughly the energy and width of the $^8$Be resonance that has been used as the intermediate state in the above $R$-matrix analyses.

### A. Dependence on resonance parameters

Variations of the two-body energy and width and subsequent computations of three-body decay require major

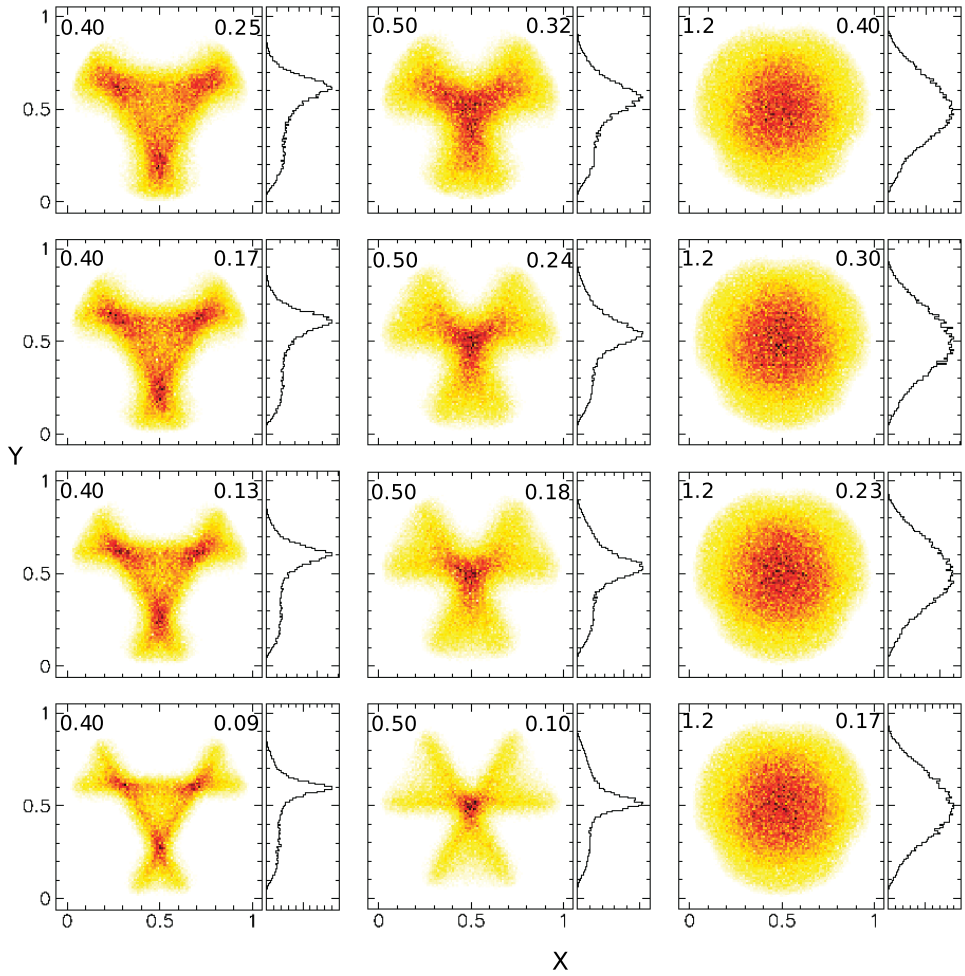


FIG. 7. (Color online) Dalitz distributions from $R$-matrix analysis for decay into three $\alpha$-particles of the $4^-$ resonance in $^{12}$C at an energy of $E_{3r} = 6.08$ MeV and a partial width of about 375 keV. The energies and widths of the intermediate $2^+$ resonance in $^8$Be are varied. $E_{2r}/E_{3r}$ is shown the left and $\Gamma_{2r}/E_{3r}$ in the right panels. The relative angular momenta between the first $\alpha$ particle and $^8$Be is $\ell_y = 3$. The coordinates are $y = E_{\alpha 1}$ and $x = \frac{E_{\alpha 1}+2E_{\alpha 2}}{\sqrt{3}} + \frac{1-\sqrt{3}}{2}$ with the energies normalized to the maximal possible $\alpha$ energy $E_{\alpha,\max} = 2E_{3r}/3$. The single-$\alpha$ energy distributions are shown as projections on the ordinate axis.

numerical work. To investigate the influence of the intermediate two-body structure with much less effort we varied instead the three-body resonance parameters. This is possible within a range of three-body energies by use of a three-body potential of varying strength. Then an increasing energy implies that the width also increases and the resonance condition cannot be fulfilled at some point when the energy exceeds the effective barrier height. These variations also imply that the changes of the relative energy $E_{2r}/E_{3r}$ and width $\Gamma_{2r}/E_{3r}$ of the two-body resonance are fully correlated as scaled by the same three-body energy.

The method of complex rotation provides a rigorous definition of sequential decay, i.e., stable population at large distances of the adiabatic potential corresponding to the intermediate two-body resonance. This state separates from all other potentials by approaching the resonance energy, whereas all other potentials converge toward zero. This state only separates out for a rotation angle larger than $\theta_{2r}$ as discussed in Sec. II A. We show the breakup energy distributions in Figs. 9 and 10 for two rotation angles where the largest angle isolates the population of the $^8$Be($2^+$) resonance in a single adiabatic potential. This contribution can then be excluded in contrast to the small angle where this two-body resonance contribution is distributed over many adiabatic potentials. Hence, for the large rotation angle we include only the direct decay into the three-body continuum. The fractions of sequential decay at large distance are given in Table I for the different values of $E_{3r}$ shown in Fig. 9.

For all three resonances the variations, amounting to about a factor of two on both energy and width, produce only relatively small but visible changes in the energy distributions. As for the $R$-matrix simulations large width and large energy both lead to less sensitivity of the distributions. With the realistic resonance parameters the distributions reproduce the measured results for the $1^+$ state; see Refs. [7,19,21].

We next attempt to investigate the connection to the basic assumption in the $R$-matrix formalism, i.e., the two-step process of two consecutive sequential decays. For the $1^+$ state only one intermediate angular momentum coupling is allowed ($\ell_y = 2$) while two $\ell_y$ values are possible for both $2^-$ and $4^-$. For the same $^8$Be structure each $\ell_y$ corresponds to one sequential decay possibility seen as two adiabatic potentials with those quantum numbers remaining finite at large distances. The three-body energy increases as we move down in the Table I and the sequential decay probability increases from essentially zero to almost 100% for all three resonances. The three-body widths increase strongly with three-body energy that indicates that the numerical accuracy could be less than desired. The increasing fraction of sequential decay is intuitively expected when the first particle can be

TABLE I. The probability $P_{\rm seq}$ for populating the component $\ell_y$ (relative angular momentum between one $\alpha$ particle and the center-of-mass of the other two) at large distances in computations of resonances with $J^\pi$ for $^{12}$C for a complex rotation of angle $\theta = 0.25$. The three-body resonance energy $E_{3r}$ and width $\Gamma$ are varied by adjusting the strength of the Gaussian three-body potential. The two-body energy $E_{2r} = 2.7$ MeV of the $^8$Be($2^+$) is maintained.

| $J^\pi$ | $E_{2r}/E_{3r}$ | $\Gamma_{2r}/E_{3r}$ | $E_{3r}$ (MeV) | $\Gamma_{3r}$(MeV) | $l_y$ | $P_{\rm seq}$ |
|---|---|---|---|---|---|---|
| | 0.86 | 0.43 | 3.5 | 0.005 | 2 | 0.001 |
| | 0.56 | 0.28 | 5.4 | 0.09 | 2 | 0.12 |
| $1^+$ | | | | | | |
| | 0.39 | 0.19 | 7.8 | 1.15 | 2 | 0.89 |
| | 0.35 | 0.17 | 8.6 | 1.85 | 2 | 0.96 |
| | 1 | 0.5 | 3.0 | 0.02 | 1 | 0.03 |
| | | | | | 3 | 0.0005 |
| | 0.75 | 0.38 | 4.0 | 0.11 | 1 | 0.19 |
| | | | | | 3 | 0.001 |
| $2^-$ | | | | | | |
| | 0.67 | 0.33 | 4.5 | 0.57 | 1 | 0.36 |
| | | | | | 3 | 0.06 |
| | 0.6 | 0.30 | 5.0 | 1.16 | 1 | 0.76 |
| | | | | | 3 | 0.1 |
| | 0.6 | 0.30 | 5.0 | 0.21 | 3 | 0.03 |
| | | | | | 5 | 0.0003 |
| | 0.5 | 0.25 | 6.0 | 1.04 | 3 | 0.71 |
| | | | | | 5 | 0.01 |
| $4^-$ | | | | | | |
| | 0.46 | 0.23 | 6.5 | 1.83 | 3 | 0.97 |
| | | | | | 5 | 0.02 |
| | 0.43 | 0.21 | 6.9 | 3.38 | 3 | 0.85 |
| | | | | | 5 | 0.007 |

emitted with a sufficiently large kinetic energy compared to the height of the corresponding barrier.

In Fig. 10 the results omitting these, sometimes large, contributions from sequential decay are shown for the large rotation angle. The distributions are qualitatively very similar to the results for the small rotation angle where the sequential decay is distributed over many adiabatic potentials. The explanation within model quantities is that essentially only one adiabatic potential contributes to the direct decay. The asymptotic large-distance angular wave function corresponding to this potential is almost independent of rotation angle. Because large distances determine the Fourier transform the energy distribution is independent of rotation angle.

That one angular wave function dominates at large distances is rigorously seen for short-range interactions where the decoupled hyperspherical wave functions asymptotically are approached. Including the repulsive Coulomb interaction could lead to strong coupling at large distance between the adiabatic potentials. However, the diagonal part of the Coulomb interactions are included in the adiabatic potentials. Furthermore, we try to use a sufficiently large basis to have a stable region of hyperradii where the asymptotics is correctly reproduced. The basis size refers to both the number of adiabatic potentials and the basis used for each of the Faddeev components. This means that an even larger hyperradius would require a larger basis to reproduce the same result. To be economic we search for a minimum basis and a stable range of hyperradii outside the interaction region [22]. Therefore we believe that the result of one adiabatic potential is at least semiquantitatively correct, but more contributions could modify the shape of the direct part of the decay. This is possible but not easily tested because level crossings are present in the critical region where the two-body resonance still couples to the other adiabatic potentials.

### B. The concept of sequential decay in three-body computations

In principle the procedure should be to compute the direct decay distribution from the complex scaled wave function and add the sequential contribution treated separately. Comparison of the results of the two rotation angles in Figs. 9 and 10 combined with the sequential decay probability in Table I immediately allows the conclusion that sequential and direct decays must be rather similar when a substantial part can be classified as sequential. Otherwise the energy distributions would depend much more on the rotation angle. The procedure could also be formulated as rotating the coordinates in the resonance wave function back to the real axis, then using Fourier transform and getting the momentum distributions that, after suitable integration over nonobserved quantities, provide the observable energy distributions. This involves numerical rotation across the singularities of the two- and three-body resonance poles, and is in general not possible without analytic expressions for the wave functions. However, when asymptotic large-distance stability is reached the total wave functions are found as hyperradial-independent linear combinations of the angular wave functions corresponding to the adiabatic potentials. Because the rotation involves only the hyperradius we have directly rotated back to the real axis for large distances. The Fourier transform depends only on the large-distance properties and we have with these assumptions in principle found the energy distributions.

However, the asymptotic two-body resonance substructure is only easily rotated back to the real axis and Fourier transformed when the Breit-Wigner expansion is used. The Breit-Wigner approximation is often much too inaccurate as seen in all the above $R$-matrix simulations. The same difficulty is not present for the other three-body wave functions corresponding to direct decay. Here the energy distributions arise almost entirely from the angular wave functions distributing the available energy between the three particles. The Breit-Wigner smearing can easily be included but has only marginal influence. Improving the treatment of the two-body sequential part necessarily must account for the asymmetries introduced by considering energies away from the resonance center. This involves detailed probabilities for populating the intermediate decaying structure as function of energy. In turn this involves the shorter distances where the couplings between the two-body resonance substructure and the other three-body states are strong. Then we are back to attempts to separate different degrees of freedom at short distances that is impossible when $\Gamma_{2r}$ is too large, as seen from Eq. (5).

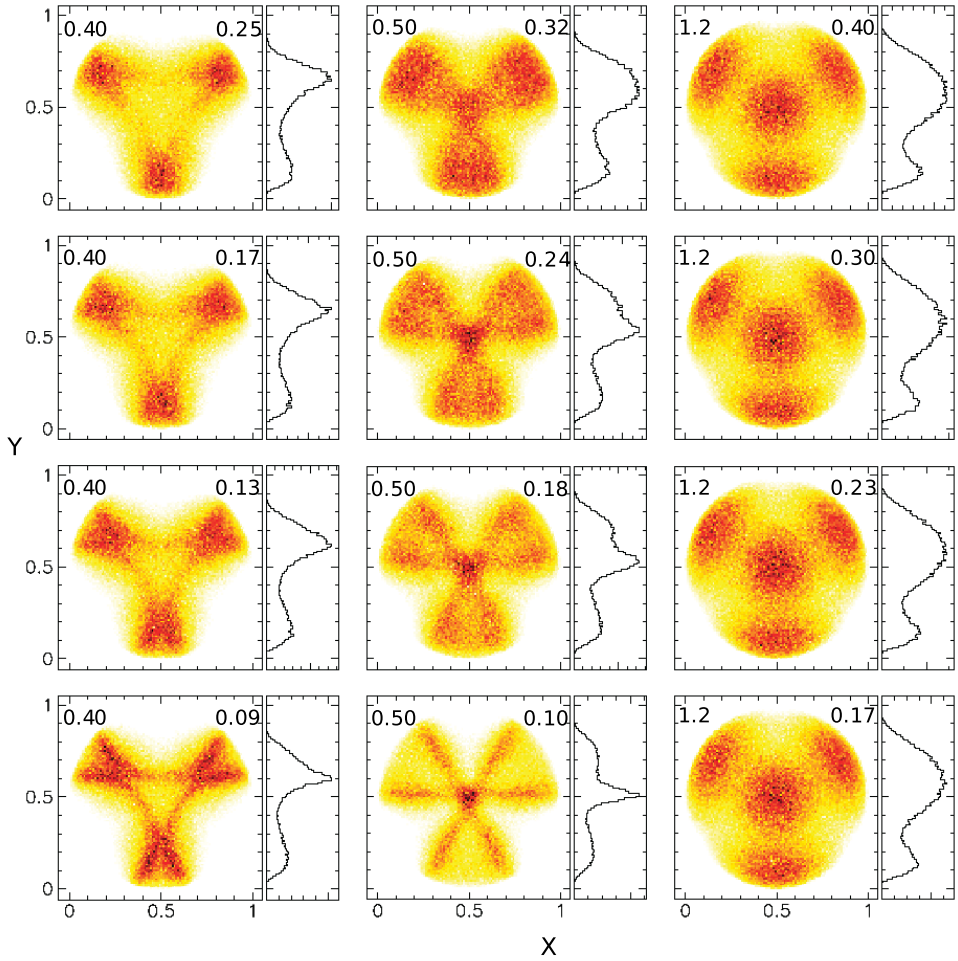


FIG. 8. (Color online) Dalitz distributions from $R$-matrix analysis for decay into three $\alpha$-particles of the $4^-$ resonance in $^{12}$C at an energy of $E_{3r} = 6.08$ MeV and a partial width of about 375 keV. The energies and widths of the intermediate $2^+$ resonance in $^8$Be are varied in the simulations. $E_{2r}/E_{3r}$ is given to the left and $\Gamma_{2r}/E_{3r}$ to the right in the panels. The relative angular momenta between the first $\alpha$ particle and $^8$Be is $\ell_y = 5$. The coordinates are $y = E_{\alpha 1}$ and $x = \frac{E_{\alpha 1}+2E_{\alpha 2}}{\sqrt{3}} + \frac{1-\sqrt{3}}{2}$ with the energies normalized to the maximal possible $\alpha$ energy $E_{\alpha,\max} = 2E_{3r}/3$. The single-$\alpha$ energy distributions are shown as projections on the ordinate axis.

Thus, to sum up, separation of the degrees of freedom related to sequential and direct decays is in principle possible when $E_{3r}$ is large compared to $\Gamma_{2r}$. Then the Breit-Wigner approximation for the sequential part is fairly accurate. Examples of this are rather abundant among the natural parity states of $^{12}$C. We have in earlier publications discussed prominent examples like the Hoyle state and the second $0^+$ resonance in $^{12}$C [7,19]. When $E_{3r}$ is too small compared to $\Gamma_{2r}$ distinction is meaningless because the degrees of freedom are completely entangled. All the resonance decay should simply be computed as direct three-body decay. This is most efficiently and accurately achieved by choosing the smallest possible rotation angle larger than $\theta_{3r}$. Larger rotation angles, in principle allowing for separation of the sequential decay branch, should not be used because a proper treatment would look like direct decay for these large widths.

## VI. RELIABILITY OF INTERPRETATIONS

Let us assume we have data from measurements and results from model computations; this is presently the case for the $1^+$ state discussed earlier. We want to extract as much information as possible about the decaying system, i.e., about initial structure and reaction or decay mechanisms. The data are first analyzed using the $R$-matrix formulations. When the two-body parameters (resonance energies, widths, and penetrabilities) are known the three-body resonance energies and widths are deduced along with the initial population as function of energy. This may be a difficult or impossible task with broad overlapping three-body resonances. There may not be a unique solution but only constraints on the parameters.

One of the deduced set of quantities is the branching ratios for the different decay paths defined by the two-body channel. This is only possible in some limits. Special care is necessary, and even when a set of parameters match the data the solution may be rather meaningless. To understand this we can vary one of the two-body resonance energies $E_{2r}$ and the related width $\Gamma_{2r}$. As seen from Eq. (5) and demonstrated in Figs. 4, 5, and 7, the resulting energy distributions remain essentially unchanged when $E_{2r}$ or $\Gamma_{2r}$ are too large. Thus it is impossible to distinguish between decay paths characterized by too large but different values of $E_{2r}$ and $\Gamma_{2r}$. Such branching ratios are therefore meaningless and so is the deduced decay mechanism. In general it is most likely that the decay is much better described as direct decay into the three-body continuum. This does not mean that the data cannot be described by sets of two-body parameters. The meaning is rather that many sets of two-body parameters are equally good and the two-body channels are effectively smeared out over three-body continuum states.

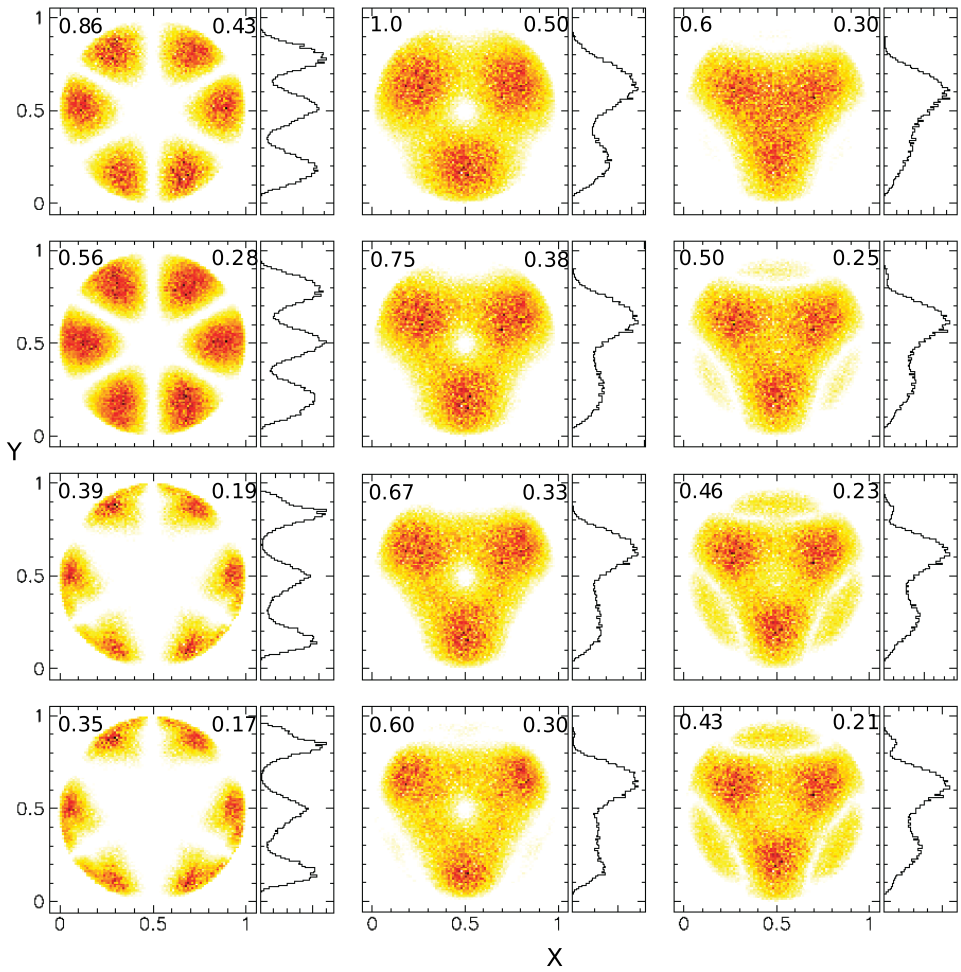


FIG. 9. (Color online) Dalitz distributions from full computation for direct decay into three $\alpha$-particles of the $1^+, 2^-, 4^-$ resonances in $^{12}$C at the measured energies of $E_{3r} = 5.43, 6.08, 4.55$ MeV, respectively (left to right columns). These energies are varied by change of the strength of the three-body potential that induces changes in the ratios $E_{2r}/E_{3r}$ and $\Gamma_{2r}/E_{3r}$. Values of $E_{2r}/E_{3r}$ are given to the left and $\Gamma_{2r}/E_{3r}$ to the right in the panels. The rotation angle is $\theta = 0.1$. The coordinates are $y = E_{\alpha 1}$ and $x = \frac{E_{\alpha 1}+2E_{\alpha 2}}{\sqrt{3}} + \frac{1-\sqrt{3}}{2}$ with the energies normalized to the maximal possible $\alpha$ energy $E_{\alpha,\max} = 2E_{3r}/3$. The single-$\alpha$ energy distributions are shown as projections on the ordinate axis.

This ambiguity in the data analysis is parallel to the distinction of decay mechanisms attempted by use of models. The complex scaling method provides in principle a mathematical definition of sequential and direct decay. However, the closer inspection in the previous sections reveals the same type of ambiguity as seen for data analysis. If $E_{2r}$ is comparable to or larger than the three-body resonance energy only virtual sequential decay is possible. This means that the three-body resonance structure at intermediate distances resembles two particles in a resonance while the third particle is farther away. When approaching the edge of the barrier the two particle must separate to conserve energy in the decay. The decay then resembles direct decay at these relatively large distances but the preferred path exploited the two-body attraction to minimize the barrier and hence maximize the decay probability. The decay products are usually better described as direct decay provided the necessary large distance properties can be accurately computed.

If $\Gamma_{2r}$ is relatively large it may still be possible to define a sequential decay probability through population at large distance of the complex scaled two-body resonance. However, this structure is defined as one pole of the Hamiltonian at a complex energy. Any deviation from this Breit-Wigner shape would be very difficult to account for. Furthermore, the large width implies a substantial extrapolation in the analytical continuation from the known properties on the real axis of the Hamiltonian. This is a major source of uncertainty for phenomenologically derived potentials as the strong interaction. In any case the large width also implies that the two-body structure is smeared out and the decay would resemble direct decay. It is then conceptually better, much simpler, and more accurate to describe as direct decay into the three-body continuum.

We have separated the process into population of a resonance, and its subsequent decay independent of the preceding history. This presupposes that a resonance is defined. Using complex scaling again assumes the one-pole approximation for each resonance, i.e., it would be difficult to improve on the Breit-Wigner approximation for the three-body resonance. That goal could be pursued without complex scaling but then the resonance definition has to be reconsidered and in addition the numerical treatment would be much more difficult already because many energies individually must be treated.

The goal for data analysis of measurements is to extract information about the decaying structure and the decay mechanism. The computations should provide matching results and derived model interpretation. This can be complicated by interference between different decay paths. The observable large-distance properties result from the dynamic evolution

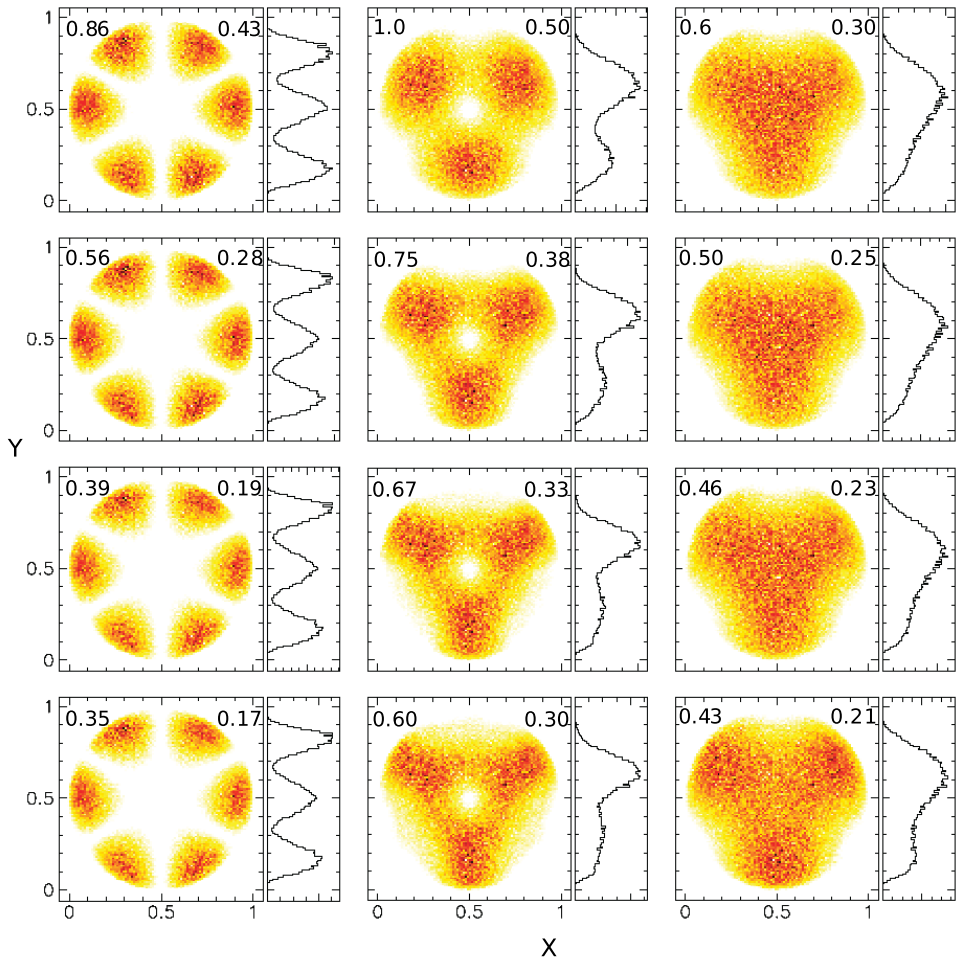


FIG. 10. (Color online) Dalitz distributions from full computation for direct decay into three $\alpha$ particles of the $1^+, 2^-, 4^-$ resonances in $^{12}$C at the measured energies of $E_{3r} = 5.43, 6.08, 4.55$ MeV, respectively (left to right columns). These energies are varied by change of the strength of the three-body potential that induces changes in the ratios $E_{2r}/E_{3r}$ and $\Gamma_{2r}/E_{3r}$. Values of $E_{2r}/E_{3r}$ are given to the left and $\Gamma_{2r}/E_{3r}$ to the right in the panels. The rotation angle is $\theta = 0.25$. Only direct decay is shown. The coordinates are $y = E_{\alpha 1}$ and $x = \frac{E_{\alpha 1}+2E_{\alpha 2}}{\sqrt{3}} + \frac{1-\sqrt{3}}{2}$ with the energies normalized to the maximal possible $\alpha$ energy $E_{\alpha,\max} = 2E_{3r}/3$. The single-$\alpha$ energy distributions are shown as projections on the ordinate axis.

that may have reorganized the small-distance structure. This evolution has to maintain the conserved quantum numbers but otherwise the small-distance structure is not directly observable.

## VII. SUMMARY AND CONCLUSIONS

The observable momentum distributions from decay of three-body resonances are analyzed by use of $R$-matrix simulations. The inherent assumptions are that the decays can be described by two successive two-body emissions. The intermediate two-body structures reached after the first emission are characterized by their energies, $E_{2r}$, and widths, $\Gamma_{2r}$. We briefly sketch the method exemplified by $3\alpha$ emission from various resonances of $^{12}$C. Because $\alpha$ particles are bosons all these states must be symmetric with respect to interchange of pairs of $\alpha$ particles. This symmetry leading to interference effects is important and accounted for in present day $R$-matrix applications.

The momentum distributions after three-body decay are calculated by $R$-matrix simulation as functions of the two-body resonance parameters. When $\Gamma_{2r}$ is small and $E_{2r}$ less than the energy of the three-body resonance the first emitted particle exhibit the corresponding Breit-Wigner distribution while the secondary emission produce broader distributions depending on the angular-momentum quantum numbers. As either $\Gamma_{2r}$ or $E_{2r}$ increase the distributions become less sensitive to their specific values.

Genuine three-body calculations are also carried out for the same systems by use of the hyperspherical adiabatic expansion method. The essential assumption is that both two- and three-body resonances are defined as complex poles in the corresponding $S$ matrices. In practice it is then difficult to go beyond the Breit-Wigner approximation for these resonances. The rigorous distinction between sequential decay via intermediate two-body states and direct decay into the three-body continuum becomes less and less meaningful both when $\Gamma_{2r}$ increases and when $E_{2r}$ increases toward and above $E_{3r}$. This precisely matches the insensitivity of the $R$-matrix analysis to these two-body parameters. The decays are then both conceptually and in practice much better described as direct decay.

We emphasize that the correct quantum statistics must be employed in $R$-matrix simulations, i.e., fermion or boson (anti-) symmetry. These symmetries are automatically included in the quantum mechanical three-body computations. We show that conserved quantum numbers as total angular momentum and parity directly are reflected in the Dalitz plots. This is most clearly seen in the probability distributions as nodes that turn out to be more abundant for unnatural than for natural parity states. These nodes are maintained from

small to large distance in the coordinate wave function and can therefore be characterized as static properties.

In general the measured momentum distributions reveal information about the initial structure of the decaying system that is tempting but misleading to interpret as a small-distance structure. It is misleading because a resonance is a quantum state where small and large distances inherently are linked together. Furthermore, the measurements reveal more directly the large-distance asymptotic structure. Extracting information of both structure and decay mechanism then require model interpretations. The $R$-matrix simulation may indicate specific branching ratios between several decay paths. Such results are reliable only when the energies and widths of the intermediate states are relatively small. Otherwise the results are insensitive to which decay path is chosen.

The pattern of nodes in the momentum distributions is strongly indicative of which angular momentum and parity should be attached to the decaying state. When many such nodes are present the corresponding symmetries control qualitatively the behavior of the measured distributions. Achieving better quantitative reproduction then requires substantially improved computations. The effects of interactions or the decay mechanism are not easily detected. This seems to be more frequent for unnatural parity states. When only very few or no nodes are present the Dalitz plots are much more indicative of the decay mechanism. This seems to be relevant for decays of natural parity states.

In summary, we compare $R$-matrix simulations with results from three-body computations. The $R$-matrix formulation inherently assumes two successive two-body emissions expressed as sequential decays. The corresponding interpretations in terms of sequential decays are meaningful only when energies and widths of the intermediate structures are small. This is also seen from three-body calculations that show that the large-distance asymptotic structures are decisive for the momentum distributions after decay. Thus, except for effects of conserved quantum numbers, small-distance many-body structure and dynamic evolution are both crucial for reliable computations. In conclusion, not all that fits make sense; parameter sensitivity combined with meaningful physical interpretation is also indispensable.

## ACKNOWLEDGMENT

This work was partially supported by the Spanish MICINN under contract FIS2008-01301.

[1] A. M. Lane and R. G. Thomas, Rev. Mod. Phys. **30**, 257 (1958).
[2] B. V. Danilin *et al.*, Sov. J. Nucl. Phys. **46**, 225 (1987).
[3] A. A. Korsheninnikov, Yad. Fiz. **52**, 1304 (1990) [Sov. J. Nucl. Phys. **52**, 827 (1990)].
[4] F. Prats and A. Salyers, Phys. Rev. Lett. **19**, 661 (1967).
[5] D. P. Balamuth *et al.*, Phys. Rev. C **10**, 975 (1974).
[6] H. O. U. Fynbo *et al.*, Phys. Rev. Lett. **91**, 082502 (2003).
[7] R. Álvarez-Rodríguez, A. S. Jensen, D. V. Fedorov, H. O. U. Fynbo, and E. Garrido, Phys. Rev. Lett. **99**, 072503 (2007).
[8] F. C. Barker, Phys. Rev. C **68**, 054602 (2003).
[9] A. J. Bartlett, J. A. Tostevin, and I. J. Thompson, Phys. Rev. C **78**, 054603 (2008).
[10] E. Nielsen, D. V. Fedorov, A. S. Jensen, and E. Garrido, Phys. Rep. **347**, 373 (2001).
[11] D. V. Fedorov, E. Garrido, and A. S. Jensen, Few-Body Syst. **33**, 153 (2003).
[12] E. Garrido, A. S. Jensen, and D. V. Fedorov, Phys. Rev. C **78**, 034004 (2008).
[13] E. Garrido, D. V. Fedorov, A. S. Jensen, and H. O. U. Fynbo, Nucl. Phys. **A766**, 74 (2005).
[14] L. C. Biedenharn and M. E. Rose, Rev. Mod. Phys. **25**, 729 (1953).
[15] R. H. Dalitz, Philos. Mag. **44**, 1068 (1953).
[16] C. Zemach, Phys. Rev. **133**, B1201 (1964).
[17] R. Álvarez-Rodríguez, E. Garrido, A. S. Jensen, D. V. Fedorov, and H. O. U. Fynbo, Eur. Phys. J. A **31**, 303 (2007).
[18] R. Álvarez-Rodríguez, H. O. U. Fynbo, A. S. Jensen, and E. Garrido, Phys. Rev. Lett. **100**, 192501 (2008).
[19] R. Álvarez-Rodríguez, A. S. Jensen, E. Garrido, D. V. Fedorov, and H. O. U. Fynbo, Phys. Rev. C **77**, 064305 (2008).
[20] W. A. Friedman, Phys. Rev. C **6**, 87 (1972).
[21] M. Alcorta, Nucl. Inst. Meth (in press).
[22] E. Garrido, D. V. Fedorov, and A. S. Jensen, Nucl. Phys. **A790**, 96c (2007).